Cent. Eur. J. Phys. • 6(3) • 2008 • 619-627
DOI: 10.2478/s11534-008-0095-0

VERSITA

Central European Journal of **Physics**

# Discreteness in time*

**Research Article**

Ulf Peschel†, Christoph Bersch, Georgy Onishchukov

*Institute of Optics, Information and Photonics (Max Planck Research Group), University of Erlangen-Nuremberg, Günther-Scharowsky-Str. 1/Bau 24, 91058 Erlangen, Germany*

**Received 14 November 2007; accepted 13 May 2008**

**Abstract:** In this paper we discuss the joint propagation of a periodically modulated field and a pulse of different frequency in an optical fiber. The pulse experiences the action of an index lattice induced via cross-phase modulation by the periodic field. We predict effects of discreteness to show up both in the temporal and in the spatial domain. For large walk-off between the two fields one should observe Bloch oscillations in frequency space, where discrete diffraction is expected to occur for equal velocities of both waves.

**PACS (2008):** 42.65.Jx, 42.65.Sf, 42.65.Wi, 42.82.Et

**Keywords:** beam trapping • self-phase modulation • dynamics of nonlinear optical systems • nonlinear waveguides • waveguide arrays



## 1. Introduction

In the past nonlinear optics was restricted to homogenous systems. Only recently it was shown that periodically modulated transverse index structures can effectively discretize continuous space, thus allowing for the observation of completely new phenomena of wave propagation and soliton formation [1]. The main aim of this paper is to discuss the transfer of respective concepts to the temporal domain. The idea is to launch a periodic field which forms an effective potential for a signal wave propagating at a different wavelength. Thus we follow a concept originally introduced by Christodoulides and co-workers to create waveguide arrays in photorefractive crystals [2]. They proposed to optically induce a photonic lattice with a writing beam having a polarization where the electro-optic effect of the crystal is minimal. Photoexcited carriers finally create a refractive-index pattern similar to the intensity distribution of the writing beam. Light launched at a wavelength different from that of the writing beam can propagate in this induced lattice. By choosing the polarization of the two interacting beams to be orthogonal, nonlinear interaction between them can be largely suppressed and the signal beam experiences an almost passive lattice. In contrast, the nonlinear self-action of the signal beam remains strong allowing for the investigation of nonlinear effects at rather low power levels. This proposal was soon realized [3] thus marking the starting point of a series of experimental investigations on discrete systems. Although impressive results have been obtained, respective experiments also suffer from certain drawbacks. The available propagation length is restricted to the size of the sample, therefore, the number of waveguides excited in respective experiments is definitively limited. In contrast, within fibers light can propagate over tens of kilo-

*Presented at 9-th International Workshop on Nonlinear Optics Applications, NOA 2007, May 17-20, 2007, Świnoujscie, Poland

†E-mail: upeschel@optik.uni-erlangen.de

meters, a span which can again be extended by several orders of magnitude by including optical amplification. In addition, time windows are basically not restricted thus providing almost unlimited space for transverse evolution. Last but not least, the fiber is one of the most developed optical systems being extremely clean and regular. Pulse propagation and spectral evolution can be monitored at comparably low costs and with extremely high precision. Although our main target is to reproduce spatial effects in the temporal domain, the controlled interaction of optical pulses in a temporal lattice could add new degrees of freedom to pulse shaping, regeneration, and processing as we will demonstrate in the following.

The paper is organized as follows: In part II we introduce the system under investigation, discussing the two rather distinct limiting cases. If there is no walk-off between signal and writing beam, we can reproduce effects known from the spatial systems. (We will discuss respective prerequisites in part III). On the contrary, large walk-off between both waves forces the signal to rapidly cross the induced index lattice. As a consequence, a regime very similar to that of a biased superlattice is established and Bloch oscillations can be observed in the spectral domain. Respective effects will be discussed in section IV. A short summary concludes the paper.

## 2. The basic scheme for discretization

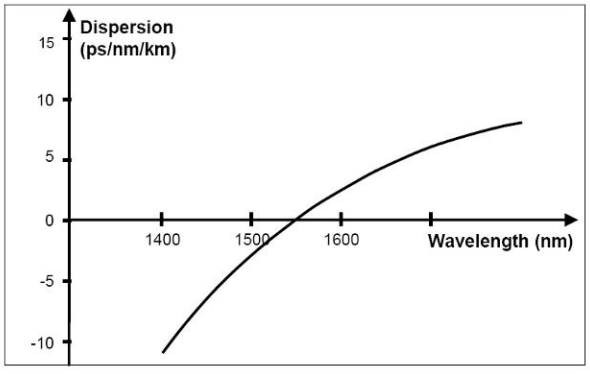


**Figure 1.** GVD of the fiber under consideration.

Our scheme is based on the nonlinear interaction between a signal $u_s$at the wavelength $\lambda_s$ and a strong periodic writing wave $u_w$ at the wavelength $\lambda_w$ with the period $T_0$. Both frequencies are well separated so that only cross-phase and self-phase modulation have to be taken into account during propagation in a single-mode fiber. Respective evolution equations are well known (see for example [4]). They read as

**Table 1.** Characteristic constants which characterize a periodic lattice.

| Type of Lattice | $N_c$ | | $N_d$ | | $\alpha$ | |
|---|---|---|---|---|---|---|
| sinusoidal | 6.9 | | 31 | | 0.043 | |
| sech $W$=0.1 | 3.8 | -4.3 | 14 | -23 | 0.10 | 0.038 |
| sech $W$=0.05 | 3.3 | -4.0 | 11 | -25 | 0.19 | 0.030 |

$$\left[i\frac{\partial}{\partial z} - \frac{D_w}{2}\frac{\partial^2}{\partial t^2} + \gamma\left(|u_w|^2 + 2|u_s|^2\right)\right]u_w = 0 \quad (1)$$

$$\left[i\frac{\partial}{\partial z} + i\Delta\frac{\partial}{\partial t} - \frac{D_s}{2}\frac{\partial^2}{\partial t^2} + \gamma\left(|u_s|^2 + 2|u_w|^2\right)\right]u_s = 0. \quad (2)$$

In above equations we have chosen a reference frame where the writing wave is at rest. Consequently, a walk-off term appears in the second equation where $\Delta$ reflects the difference of the inverse group velocities of the interacting waves. $D_w$ and $D_s$ account for the group velocity dispersion (GVD) at both frequencies, respectively, and we regard the effective nonlinear coefficient $\gamma$ to be frequency-independent. In what follows we always refer to parameters of a commercially available highly nonlinear fiber ($\gamma = 10\ W^{-1}\ \mathrm{km}^{-1}$) having its zero-dispersion point in the middle of the C-band at $\lambda$=1546 nm (see Fig. 1). Hence, by varying the wavelength of the writing and the signal wave different situations, with respect to the strength of walk-off and the sign of the GVD, can be realized without leaving the gain area of Er-doped amplifiers. Although the losses in the fiber under consideration are extremely low (0.8 dB/km), additional amplification is required if propagation distances exceed 3 km.

One essential prerequisite of the following considerations is that the effective potential formed by the writing beam remains stationary. Of course the writing beam is subject to dispersive spreading and nonlinear evolution. In what follows we intend to give a few and rough estimates on critical propagation distances above which the evolution of the writing beam starts to play a role.

All linear evolution is driven by GVD. Its absolute value will never exceed 1.5 $\mathrm{ps}^2$/km if we focus onto our highly nonlinear fiber and restrict to the C-band (see Fig. 1). In the low-power case every periodic field will recover after a Talbot length $L_T$ which thus defines a critical scale of a linear evolution. Assuming a period of $T_0$=25 ps and a maximum GVD, the Talbot length yields

$$L_T = \frac{T_0^2}{\pi|D|} = 132.6\ \mathrm{km}. \quad (3)$$

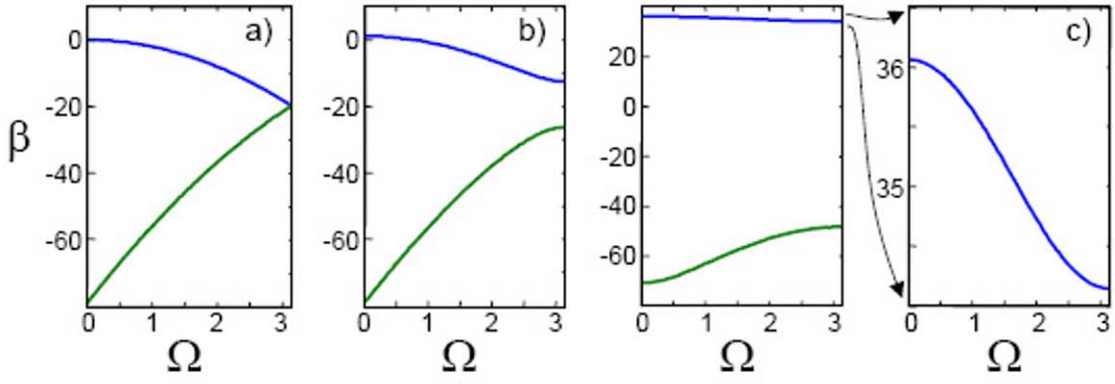


**Figure 2.** Band structures of particles in a sinusoidal potential of varying depth a) $N_0$=0 (free particle), b) $N_0 = N_c$=6.9, c) $N_0 = N_d$ =31 (the first band is magnified to illustrate its cosine-like structure).

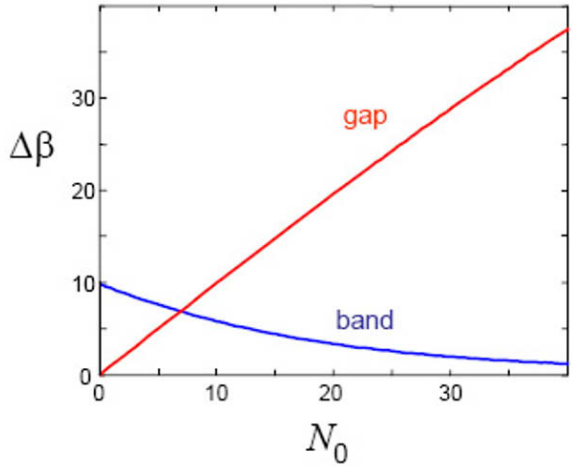


**Figure 3.** Width of the first band and of the first gap depending on the strength of the sinusoidal potential.

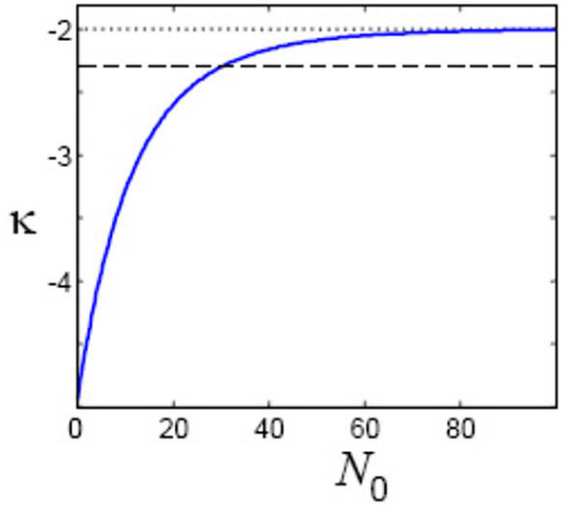


**Figure 4.** Ratio $\kappa$ between the size of the band and the value of the second derivative as a function of the strength of a sinusoidal lattice (dashed line: 10% deviation from the discrete limit, dotted line: discrete limit).

However, smaller substructures of the periodic field can evolve much faster. In contrast, a sinusoidal field, on which we will focus in the following, will not evolve as long as nonlinear effects can be neglected.

It is much harder to estimate the influence of nonlinear effects. A typical nonlinear length-scale $L_{NL}$ is given by the distance where the nonlinearly induced phase shift reaches $2\pi$. For the fiber under consideration and an average power of 5 mW the nonlinear length amounts to 126 km. Hence, respective distances are of the same order as linear evolution. However, a nonlinearly induced phase shift need not result in a modified intensity distribution. Only the joint action of non-vanishing GVD and nonlinearity will result in a deformation of the potential. In any case the influence of the nonlinearity will limit the validity of our model. Special schemes might be required to limit the influence of nonlinear effects on the periodic field. In what follows we will always include the evolution of the writing beam into the numerical simulations.

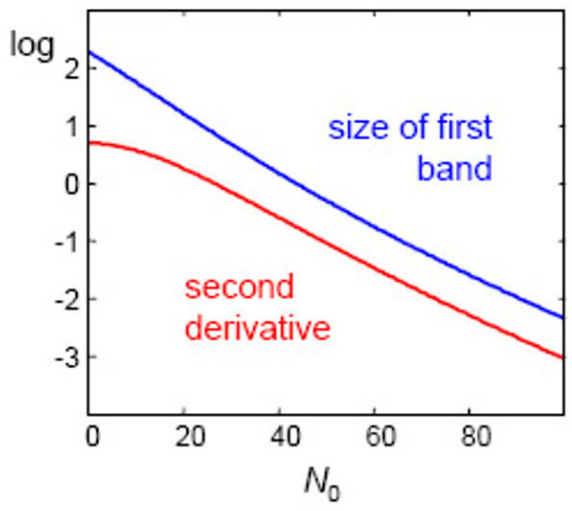


**Figure 5.** Logarithmic plot of the size of the first band and of the value of the second derivative in the center of the Brillouin zone.

## 3. Discrete behavior in periodic temporal potentials

Our intention is to form a time-periodic effective potential whereby a signal pulse can propagate. We now determine the required strength of this potential, i.e. of the writing wave, by assuming the writing wave does not evolve during propagation and compute the eigenstates of the resulting effective potential. These eigenstates are Bloch modes and define the linear propagation of the signal wave. Based on these findings we discuss prerequisites for an effective discretization of the system.

We assume the signal to be influenced only by the power of the writing wave $p(t) = |u_w|^2$ and neglect the self-phase modulation of the signal wave. We end up with

$$\left[ i\frac{\partial}{\partial z} + i\Delta\frac{\partial}{\partial t} - \frac{D_s}{2}\frac{\partial^2}{\partial t^2} + 2\gamma\, p(t) \right] u_s = 0. \qquad (4)$$

A frequency transformation

$$u_s(t) = \tilde{u}_s(t) \cdot \exp\left[ -i\left( \bar{\omega}\, t - \frac{D_s}{2}\bar{\omega}^2 z \right) \right] \quad \text{with} \qquad (5)$$
$$\bar{\omega} = -i\frac{\Delta}{D_s}$$

is used to remove the walk-off term. We basically shift our spectral reference to the point where the group velocities of signal and writing wave coincide. As long as Eq. (4) is valid such a transformation can always be performed, however, it need not yield a useful result. First, the resulting frequency might coincide with that of the writing beam making both waves indistinguishable. Secondly, if the deduced frequency shift is too big third order dispersion has to be taken into account in Eq. (4), thus changing the result of Eq. (5). Hence, one should always check on the basis of the complete dispersion relation of the fiber, whether one has really found a point of equal group velocities of signal and writing waves. In the case of the fiber investigated here (see Fig. 1), the frequencies of signal and writing waves must be placed symmetrically on opposite sides of the zero-dispersion point.

As stated above $p(t)$ is periodic with a fixed period $T_0$ defining a natural time scale and a respective normalization. The normalized equation now reads as:

$$\left[ i\frac{\partial}{\partial Z} + \frac{\partial^2}{\partial T^2} + N_0 g(T) \right] \tilde{u}_s = 0 \quad \text{with} \qquad (6)$$
$$T = \frac{t}{T_0}, \quad Z = \frac{z}{Z_0} \text{ and } \quad Z_0 = -2\frac{T_0^2}{D_s}.$$

We have also introduce an effective strength $N_0$ of the periodic potential,

$$N_0 = -\frac{4\gamma T_0^2}{D_s} P_0 \quad \text{with} \quad P_0 = \frac{1}{T_0}\int_0^{T_0} dt\, p(t) \qquad (7)$$

where $P_0$ is the averaged power of the periodic field. Depending on the GVD $N_0$ is either positive or negative, but its absolute value can be tuned by changing the power of the writing beam. Due to our normalization $g(T) = \frac{1}{P_0} p(T)$ which is a periodic function with a period of 1 and an averaged power of 1.

Eigenstates of the periodic potential are Bloch waves of the form

$$\tilde{u}_s(T) = U(T) \exp\left[ i(\beta Z - \Omega T) \right] \qquad (8)$$

where $U(T)$ is a lattice-periodic function. $\Omega$ plays the role of a Bloch vector and is restricted to the interval $[-\pi, \pi]$. Note that due to our focus on temporal effects it appears to be a frequency. To determine $\beta(\Omega)$ we solve the eigenvalue problem

$$\left[ \frac{\partial^2}{\partial T^2} + 2i\,\Omega\frac{\partial}{\partial T} - \Omega^2 + N_0 g(T) \right] U = \beta(\Omega)\; U. \qquad (9)$$

Let us first consider the general form of the band structure. In case of a free particle ($N_0 = 0$) the first band extends

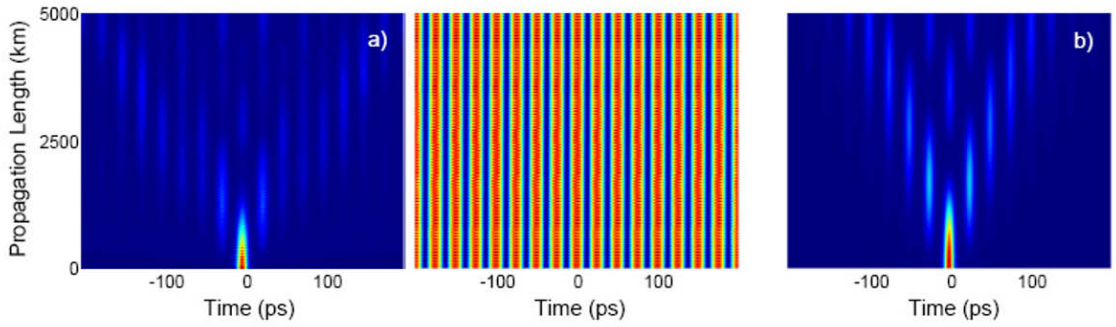


**Figure 6.** Discrete temporal diffraction in a sinusoidal lattice (parameters in the text) a) signal (left) and writing wave (right) are both subject to nonlinear action, b) signal wave for a fixed periodic potential.

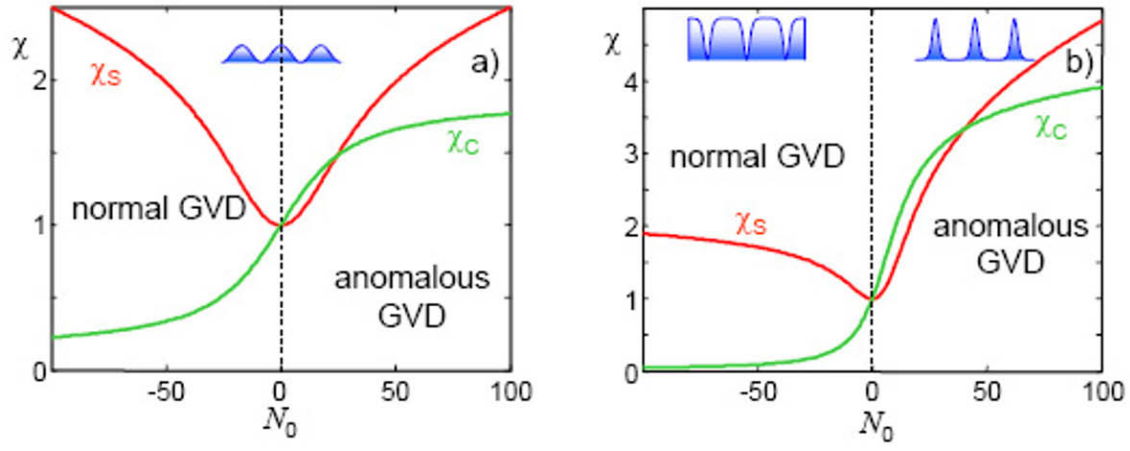


**Figure 7.** Effective nonlinear self-phase modulation of the signal wave $\chi_S$ and the strength of its interaction with the lattice $\chi_C$ for a sinusoidal (a) and a sech-like lattice (b) for normal ($N_0 < 0$) and anomalous ($N_0 > 0$) GVD at the signal wavelength.

between 0 and $-\pi^2$ (see Fig. 2a). Hence, its width is $\pi^2$ and the second derivative in its center yields the value $\frac{\partial^2\beta}{\partial\Omega^2}\Big|_{\Omega=0} = -2$. As soon as the lattice appears for finite $N_0$, a gap opens up between the first and the second band (see Fig. 2b and Fig. 3). If this gap exceeds the size of the first band ($N_0 \geq N_c$), excitations of the first band remain restricted to it and a tight-binding approximation can be applied. Increasing the energy of the lattice even further reduces the interaction between the sites. Finally, each potential minimum interacts with its nearest neighbors only. We have approached the discrete limit, where the band structure is given by $\beta(\Omega) = 2C\cos(\Omega)$ with the coupling constant to nearest neighbors $C$ (see Fig. 2c). In that limiting case the size of the band is $4C$ and the second derivative $\frac{\partial^2\beta}{\partial\Omega^2}\Big|_{\Omega=0} = -2C$. The ratio $\kappa(N_0)$ between the size of the band and the value of the second derivative tells us how close we are to the discrete limit. Its limiting cases are that for the free particle $\kappa(0) = -\frac{\pi^2}{2}$ and the discrete limit $\kappa(\pm\infty) = -2$ (see Fig. 4). As can be seen in Fig. 5, both the size of the gap as well as the second derivative in its center depend exponentially on the strength of the lattice. Both quantities become quickly correlated by a fixed factor marking the approach of the discrete limit. In that limit the coupling constant $C$, which is proportional to the width of the band and to the second derivative in its center, depends exponentially on the lattice strength as well. This is obvious because coupling is mediated by the overlapping evanescent field tails trapped in adjacent potential minima. Evanescent fields are known to depend exponentially on the strength of the potential in which they penetrate.

Here we characterize different lattices by three constants:

- $N_c$: the value of the lattice strength where the size of the first band and of the gap coincide. From that on the evolution is dominated by a single band.

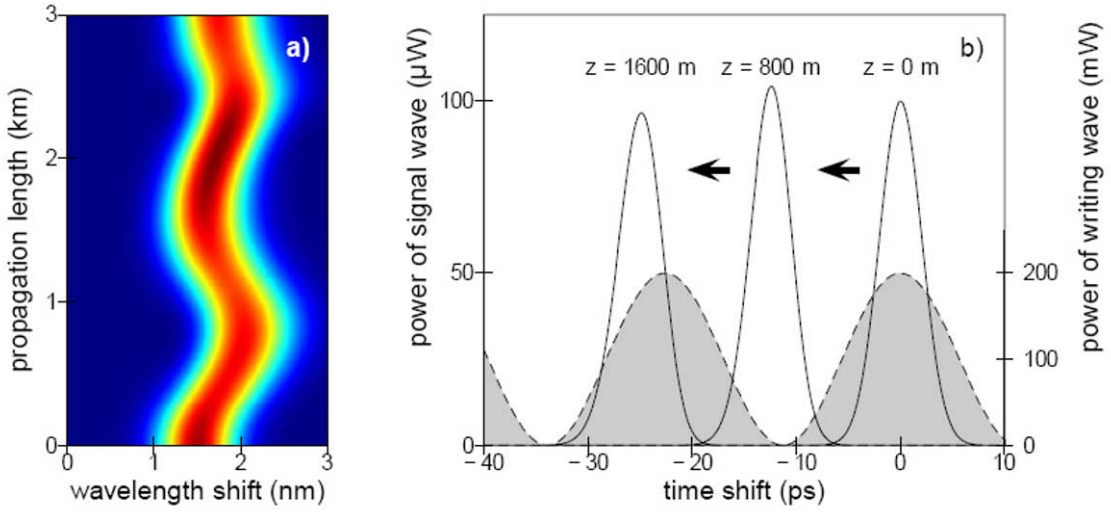


**Figure 8.** Bloch oscillations performed by a signal pulse in the spectral domain (a) correspond to a periodic interaction between signal pulse and writing wave in the temporal domain (b) (full line: signal pulses, gray area: writing wave).

- $N_d$: the value of the lattice strength where $\kappa$ deviates less than 10% from the difference between the initial deviation (free particle, $N_0 = 0$) and its final value (infinite potential, $N_0 = \infty$). It gives an estimate for a lattice strength from that on the evolution is dominated by nearest neighbor interaction.

- $\alpha$: the exponential dependence of the coupling constant on the strength of the lattice $C \approx C_0 \exp(-\alpha\ |N_0|)$.

Obviously, the transition from free-particle behavior to the discrete case is continuous. $N_c$ an d$N_d$ can only help to estimate its dependence on the lattice strength but should not be understood as strict transition points.

Note that in the case of normal GVD $N_0$ is negative. Here we compare two types of lattices: the sinusoidal lattice $g(T) = 1 + \cos(2\pi\ T)$ and the sech-shaped one. The latter consists of a sequence of single pulses $g(T) \propto \cosh^{-2}(T/W)$ each one being restricted to a single interval of the periodic lattice (see Table 1). While the sinusoidal lattice is not influenced by a change of sign of $N_0$ the sech-shaped potentials are much less effective for negative values of $N_0$. For a signal propagating in the normal GVD regime, the pulses of the writing beam repel the signal field. Consequently, the eigenstates are located between the pulses.

Having understood the normalized system Eq. (6), we can now return to real physical quantities. To successfully observe discrete temporal diffraction $N_0 \geq N_d$ should hold. This expression translates to real quantities as

$$\left|\frac{4\gamma T_0^2}{D_s} P_0\right| \geq N_d \tag{10}$$

where $N_d$ depends on the type of lattice chosen. In addition, sufficient linear temporal diffraction must be ensured. The signal pulse should spread over several wells, say at least $M$, to both sides. Hence, the propagation length, in normalized units, must be at least $M/2\ C^{-1,}$ where $C$ is the coupling constant in normalized units [6]. In real units this results in

$$L \geq M \frac{T_0^2}{|D_s|}\ \frac{1}{C(N_0)}. \tag{11}$$

To give an example we have chosen the wavelength of signal and writing beam symmetrically with respect to the zero-dispersion point at $\lambda_s$=1566 nm and $\lambda_w$=1526 nm resulting in a GVD at the signal wavelength of $D_S = -1.46$ ps$^2$/km. The sinusoidal potential should be generated with 40 GHz which corresponds to a time constant of $T_0$=25 ps. We choose a potential strength of $N_0 = N_d = 31$ for which the required averaged power of the periodic field accounts to $P_0 = \frac{N_0|D_s|}{4\gamma T_0^2} = 1.8$ mW.

For this value of $N_0$ the normalized coupling amounts to $C(N_0 = N_d) = 0.47$. Consequently, the coupling constant between adjacent wells $c$ is given by

$$c = C(N_0)\ \frac{|D_s|}{2T_0^2} = 0.55\ \cdot 10^{-6}\ \text{m}^{-1}. \tag{12}$$

To spread over 10 sites ($M = 5$) of a lattice a propagation length of about 5000 km is required (see Fig. 6). Hence, to

observe signatures of discrete behavior rather long propagation distances are required making an intermediate amplification compulsory. On the contrary, the required strength of the writing beam is surprisingly low. Still its nonlinear evolution is noticeable (see right plot in Fig. 6a). Even if absorption is completely compensated, the phase of the periodic writing beam still oscillates during propagation, which also has some impact on the temporal spreading of the signal wave (compare left plot in Fig. 6a and Fig. 6b). Fig. 6b displays the temporal diffraction pattern in a stationary lattice for comparison. Improvement can be obtained by stabilizing the writing beam by, for example, removing nonlinearly induced frequency components by additional filtering.

Having discussed the linear coupling we now deal with the nonlinear effects. The nonlinear self-action of the signal field slightly depends on the chosen eigenstate. However, when approaching the weak-coupling limit it becomes independent of the respective Bloch frequency. We choose the state with Ω=0 to evaluate the respective overlap integral as

$$\chi_s = \frac{\int_0^1 dT\ |u_s(T)|^4}{\left(\int_0^1 dT\ |u_s(T)|^2\right)^2}. \qquad (13)$$

Any nonlinear perturbation of the lattice caused by the signal pulse scales proportional to

$$\chi_c = \frac{\int_0^1 dT\ g(T)\,|u_s(T)|^2}{\int_0^1 dT\ |u_s(T)|^2 \int_0^1 dT\ g(T)}. \qquad (14)$$

Both quantities depend on the field structure of the Bloch function and, therefore, on the strength of the lattice (see Fig. 7). In the case of the free particle both quantities amount to 1. For increasing lattice strength both grow but self-interaction prevails against lattice distortions. Lattice distortions are much less pronounced for a signal wave propagating in the normal dispersion regime ($N_0$ <0). In that case the signal field is repelled from the writing beam. Coming back to our example designed for a sinusoidal lattice at $N_0 = N_d$ we notice that the scaled coefficient of self-phase modulation amounts to $\chi_s(N_d) = 1.44$. We can now formulate a Discrete Nonlinear Schrödinger equation to describe the field propagation within the potential as

$$\left(i\frac{d}{dz} + \gamma_{eff}\,|a_n|^2\right) a_n + c\,(a_{n-1} + a_{n+1}) = 0 \qquad (15)$$

with $|a_n|^2$ being the energy trapped in the nth potential minimum. The coupling constant amounts to $c = 1.62 \times 10^{-3}$ km$^{-1}$ and the effective nonlinear coefficient to $\gamma_{eff} = \frac{\gamma\chi_s}{T_0} = 5.8 \times 10^{11}$ km$^{-1}$ W$^{-1}$ s$^{-1}$.

To excite a discrete soliton, energy of the order of $c/\gamma_{eff} =$ 2.8 fJ is required which is still more than 30 times less than the energy carried by the lattice within one period. Hence, the back action on the lattice should be negligible. Finally, we want to address the question of walk-off again. We have removed it by shifting the frequency where, of course, an injected field is not affected by this transformation. If its group velocity does not match that of the writing beam it will move across the potential like a beam injected under oblique incidence into a waveguide array [5]. Hence, the frequency detuning $\bar{\omega}$ defines the Bloch frequency of the excited eigenstate Ω like

$$\Omega = \mathrm{mod}\,[\bar{\omega}T_0 + \pi]_{2\pi} - \pi. \qquad (16)$$

The identification of the excited band is not straight forward. Only in the case of the free particle a unique expression exists given by

$$m = \left|\frac{\bar{\omega}T_0 - \Omega}{2\pi}\right| + 1. \qquad (17)$$

For a non-vanishing potential frequency mixing occurs. However, we can anticipate that Eq. (17) is still valid for potentials that are not too strong. If we focus on the first band, we have to choose the frequency of the signal beam within a limited frequency domain around the point of zero walk-off to obey $|\bar{\omega}T_0| < \pi$. The frequency of the signal pulse must not deviate from the point of velocity matching more than half of the frequency of the lattice.

If walk-off is bigger, higher-order bands are excited and the effect of the periodic potential diminishes. But, as we will see in the next section, interesting effects still occur.

## 4. Bloch oscillations for large walk-off

The case of vanishing walk-off between signal and writing waves can only be realized for certain choices of the frequencies of the exciting waves. In all other cases walk-off between the two waves is so strong that it dominates the whole evolution of the signal beam. In what follows we will discuss just this case. The power distribution in the writing wave should be periodic. For simplicity we assume a cosine shape as $|u_w|^2 = P_0[\cos(\delta\omega\, t) + 1]$. In what follows all numerical simulations are based on the complete system of Eqs. (1)-(2) assuming the following set of parameters: A 40 Gbit/s pulse sequence at $\lambda_s$ = 1566 nm with a peak power of 0.1 m W and a

pulse duration (FWHM) of 4 psinteracts with a writing wave with the averaged power $P_0 = 200$ mW, a modulation period of $T_0 = 2\pi/\delta\omega = 25$ps at the wavelength of $\lambda_w = 1546$ nm in the highly non-linear fiber having the zero-dispersion point at the writing wavelength $\lambda_w$. Hence, $D_w$ is negligible and $D_s = -1.46$ ps$^2$/km is anomalous. For this choice of parameters the walk-off term in Eq. (2) amounts to $\Delta = -15.6$ ps/km.

Note that in contrast to the last section we now assume a much higher power of the writing beam to enhance the investigated effects. To allow for an analytical treatment we assume this power distribution to remain constant, an assumption which is well satisfied for short propagation distances or small values of the GVD. Of course in all numerical treatment the evolution of the complete set of dynamical equations (1-2) is solved taking into account the evolution of the writing beam as well. For propagation distances shorter than the dispersion length of the signal pulse and sufficiently high group-velocity difference, the walk-off term in Eq. (2) becomes dominant compared to the influence of GVD. Hence, the latter one will be neglected in the following analytical treatment. In addition, the signal is assumed to be weak compared to the writing wave. Thus, its self-phase modulation can be neglected compared to the cross-phase modulation induced by the writing wave. Under these assumptions Eq. (2) reads as follows:

$$\left\{ i\frac{\partial}{\partial z} + i\Delta\frac{\partial}{\partial t} + 2\gamma P_0\left[\cos\left(\delta\omega\, t\right) + 1\right]\right\} u_s = 0. \qquad (18)$$

Due to the walk-off the signal is permanently drawn across the cosine potential. During this process the actual phase of the signal must change giving rise to a periodic frequency shift. This process becomes even more evident if the Fourier transform of Eq. (18) with respect to time is performed as $U_S(\omega) = \frac{1}{2\pi}\int_{-\infty}^{+\infty} dt\; u_s(t)\; \exp(i\omega t)$:

$$\left[ i\frac{\partial}{\partial z} + \omega\Delta + 2\gamma P_0\right] U_s(\omega) + \gamma\, P_0\left[U_s(\omega-\delta\omega) + U_s(\omega+\delta\omega)\right] = 0. \qquad (19)$$

Obviously the evolution of the signal takes place in distinct subsets of an equally spaced spectral ladder. By defining a basic frequency $\omega_0$, Eq.(19) can be rewritten as a set of evolution equations for the discrete spectral amplitudes

$$a_n(z) = U_s(\omega_0 + n\;\delta\omega,\; z)\exp\left[-i\left(\omega_0\Delta + 2\kappa\right)z\right]$$
$$\left[ i\frac{\partial}{\partial z} + \alpha\, n\right] a_n + \kappa\left[a_{n+1} + a_{n-1}\right] = 0 \quad \text{with} \qquad (20)$$
$$\alpha = \Delta\delta\omega \quad \text{and} \quad \kappa = \gamma P_0.$$

In what follows we take advantage of the fact that Eq. (20) describes likewise photonic Bloch oscillations in a coupled waveguide array (coupling constant $\kappa$ and effective index gradient $\alpha$) [7–9]. An important property of the solutions of Eq. (20) is that arbitrary field distributions recover after a Bloch period of

$$z_B = 2\pi/\alpha = 2\pi/\delta\omega\Delta = T_0/\Delta. \qquad (21)$$

Within this propagation distance the pulse just passes one ripple of the writing wave. Note that this is independent of the power of the writing wave. For the above parameters this distance amounts to 1600 m.

Exactly this behavior is reproduced by numerical simulations based on Eqs. (1)-(2) (see Fig. 8). In the temporal domain each Bloch oscillation corresponds to a motion of the signal in the periodic potential by one period. The spectral intensity of the signal remains localized during the oscillation provided that several frequency components of the periodic wave are initially excited, i.e. the signal pulses have to be short compared to the modulation period of the writing wave. In this case the well-confined signal field performs oscillations in the spectral domain. According to [7] the overall elongation amounts to roughly $n_B \approx 4\kappa/\alpha$ steps of the frequency ladder. This corresponds to a wavelength shift of

$$|\delta\lambda| \approx \left|2P_0\,\lambda_S^2\,\gamma/(\pi\cdot\Delta\cdot c_L)\right| \qquad (22)$$

where $c_L$ is speed of light. For our example the maximum wavelength shift amounts to roughly 0.6 nm. Hence, by changing the power and the modulation frequency of the writing wave both the maximum wavelength shift as well as the required propagation distance can be varied separately.

Whether the oscillation starts with a frequency up- or down-shift depends solely on the initial position of the signal pulse with respect to the slope of the writing wave. In the case where the interaction starts in an intensity minimum of the periodic potential, and for a negative group-velocity difference $\Delta$, we observe an initial red shift and vice versa.

Some approximations have been made to allow for this analytical treatment, however, none of these are really critical. Because only a short propagation distance of half a Bloch period is required, effects of GVD or the nonlinear self-action of the writing wave can be neglected, as demonstrated in the numerical simulations of the complete system of Eqs. (1)-(2).

## 5. Conclusions

In conclusions we have demonstrated that the concept of discrete systems can be successfully transferred to the temporal domain. A periodic amplitude-modulated writing wave acts as an effective periodic potential for a signal pulse propagating in a highly nonlinear fiber at a different wavelength. We showed that for negligible walk-off self-interaction prevails against lattice distortions, and we were able to numerically observe discrete diffraction in time. For large walk-off between signal and writing wave we derived equations equivalent to those describing photonic Bloch oscillations. Spectral oscillations with a constant period appear for the signal field distribution.

### References

[1] D.N. Christodoulides, F. Lederer, Y. Silberberg, Nature 424, 817 (2003)
[2] N.K. Efremidis, S. Sears, D.N. Christodoulides, J.W. Fleischer, M. Segev, Phys. Rev. E 66, 046602 (2006)
[3] J.W. Fleischer, M. Segev, N.K. Efremidis, D.N. Christodoulides, Nature 422, 147 (2003)
[4] G.P. Agrawal, Nonlinear fiber optics (Academic Press, 4th ed, 2007)
[5] R. Morandotti, U. Peschel, J.S. Aitchison, H.S. Eisenberg, Y. Silberberg, Phys. Rev. Lett. 83, 2726 (1999)
[6] T. Pertsch, T. Zentgraf, U. Peschel, A. Bräuer, F. Lederer, Phys. Rev. Lett. 88, 093901 (2002)
[7] U. Peschel, T. Pertsch, F. Lederer, Opt. Lett. 23, 1701 (1998)
[8] R. Morandotti, U. Peschel, J.S. Aitchison, H.S. Eisenberg, Y. Silberberg, Phys. Rev. Lett. 83, 4756 (1999)
[9] T. Pertsch, P. Dannberg, W. Elflein, A. Bräuer, F. Lederer, Phys. Rev. Lett. 83, 4752 (1999)